Robust *in vivo* gene transfer into adult mammalian neural stem cells by lentiviral vectors

Antonella Consiglio*†‡, Angela Gritti†§, Diego Dolcetta*, Antonia Follenzi*¶, Claudio Bordignon*‖, Fred H. Gage, Angelo Luigi Vescovi§††, and Luigi Naldini*‖††**

*San Raffaele Telethon Institute for Gene Therapy, §Institute for Stem Cell Research, and ‖Vita Salute San Raffaele University, H. San Raffaele Scientific Institute, Via Olgettina 58, 20132 Milan, Italy; and **Laboratory of Genetics, The Salk Institute for Biological Studies, 10010 North Torrey Pines Road, La Jolla, CA 92037

Edited by Inder M. Verma, The Salk Institute for Biological Studies, La Jolla, CA, and approved August 23, 2004 (received for review June 16, 2004)

Stable genetic modification of adult stem cells is fundamental for both developmental studies and therapeutic purposes. Using *in vivo* marking studies, we showed that injection of lentiviral vectors (LVs) into the subventricular zone of the adult mouse brain enables efficient gene transfer into long-term self-renewing neural precursors and steady, robust vector expression in their neuronal progeny throughout the subventricular zone and its rostral extension, up to the olfactory bulb. By clonal and population analysis in culture, we proved that *in vivo*-marked neural precursors display self-renewal and multipotency, two essential characteristics of neural stem cells (NSCs). Thus, LVs efficiently target long-term repopulating adult NSCs, and the effect of the initial transduction is amplified by the continuous generation of NSC-derived, transduced progeny. LVs may thus allow novel studies on NSCs' physiology *in vivo*, and introduction of therapeutic genes into NSCs may allow the development of novel approaches for untreatable CNS diseases.

Restricted regions of the adult vertebrate brain retain neural stem cells (NSCs) that generate new neurons (1–5). Two major stem cell compartments are the subventricular zone (SVZ) of the lateral ventricles (6, 7) and the subgranular layer of the hippocampus (8–10). NSCs in the rodent SVZ generate neuroblasts, which migrate in tangentially oriented chains [the rostral migratory stream (RMS)] to the olfactory bulb (OB), where they replace interneurons (11–14). NSCs within the subgranular layer generate new granule neurons that incorporate into the dentate gyrus (15, 16). Self-renewal and multipotency of SVZ- and subgranular layer-derived NSCs have been demonstrated by *in vitro* culture (17–21).

The factors responsible for maintaining an active germinal niche in the adult brain and the signals regulating the proliferation, migration, and differentiation of the precursors are largely unknown. Multiciliated ependymal cells have been identified as the neurogenic stem cells (22), but recent evidence identified NSCs as a subset of subependymal astrocyte-like cells (B cells) (5, 6, 23, 24). B cells are primary precursors that generate transit-amplifying secondary precursors (C cells), which give rise to neuroblasts (A cells) migrating to the OB (25, 26). Neurogenesis in the dentate gyrus increases in response to external stimulation, suggesting a role in learning processes (27, 28). A variety of insults to the brain induce the proliferation of immature neurons in both the SVZ and the subgranular layer (29–31). However, whether newly generated cells integrate into functional brain circuitry has remained unclear until recently (32, 33). Astrocytes from the hippocampus have been shown to instruct NSCs to adopt a neural fate (34), and several growth factors that influence NSC *in vitro* have been reported to affect the proliferation, migration, and fate of endogenous NSCs when administered *in vivo* (35–38). How these processes are integrated *in vivo* and perturbed by pathology remain crucial areas of investigation.

These findings raise the attractive possibility that adult neurogenesis might be exploited to repair the injured brain. Such an approach requires new strategies capable of modifying the activity of endogenous precursors, which might be recruited to areas of damage, where they should functionally integrate to replace dead cells. Furthermore, endogenous progenitors may be genetically modified *in vivo* to compensate for inherited deficiencies or to steer their differentiation down specific differentiation pathways. Infusion of transforming growth factor-α into the caudate-putamen of parkinsonian rats has been shown to cause proliferation and migration of forebrain progenitors toward the infusion site, where they differentiated into neurons (39). More recently, functional hippocampal pyramidal neurons were shown to regenerate after ischemic brain injury by recruitment of endogenous progenitors mediated by growth factor administration (40). In this context, the use of lentiviral vectors (LVs) to obtain sustained expression of therapeutic genes in different neural cell populations *in vivo* (41–45) is particularly relevant.

Here, we report that advanced-generation LVs allow for efficient long-term marking of self-renewing SVZ precursors *in vivo* and stable transgene expression in their progeny throughout the SVZ-RMS-OB system. Using *ex vivo* analysis we prove clonal expansion and multipotency of the *in vivo*-marked precursors, thus showing that they display the functional features of bona fide NSCs.

Materials and Methods

Vector Production and *in Vivo* Transduction. High-titer vesicular stomatitis virus-pseudotyped LV were produced in 293T cells by transient transfection of the transfer vector pRRL-SIN-PPT-hPGK-GFP-WPRE, the late-generation packaging construct pCMVΔR8.74 and the vesicular stomatitis virus envelope-expressing construct pMD2.G, and purified by ultracentrifugation as described (46). Expression titers, determined on HeLa cells by fluorescence-activated cell sorter (FACS) analysis (FACSCalibur, Becton Dickinson), were 5×10^9 to 1×10^{10} transducing units/ml with an average HIV-1 p24 concentration of 100 μg/ml. For vector injection, 6-week-old C57/BL6 mice were used. One microliter of vector concentrate was injected by a 33G Hamilton syringe (0.2 μl/min). Stereotactic coordinates (mm from bregma): SVZ, anterior-posterior (AP) = +0.6,

This paper was submitted directly (Track II) to the PNAS office.

Freely available online through the PNAS open access option.

Abbreviations: NSC, neural stem cell; SVZ, subventricular zone; RMS, rostral migratory stream; OB, olfactory bulb; LV, lentiviral vector; FGF2, basic fibroblast growth factor; FACS, fluorescence-activated cell sorter; GFAP, glial fibrillary acidic protein; DAPI, 4,6-diamidine-2-phenylindole dihydrochloride; GCL, granule cell layer; MFI, mean fluorescent intensity.

†A.C. and A.G. contributed equally to this work.

‡Present address: Laboratory of Genetics, The Salk Institute for Biological Studies, 10010 North Torrey Pines Road, La Jolla, CA 92037.

¶Present address: Department of Medicine and Pathology, Marion Bessin Liver Research Center, Albert Einstein College of Medicine, Ullmann 625, 1300 Morris Park Avenue, Bronx, NY 10461.

††To whom correspondence may be addressed. E-mail: vescovi.angelo@hsr.it or naldini.luigi@hsr.it.

mediolateral (ML) = +1.2, and dorsoventral (DV) = −3 from the skull surface; hippocampus, AP −1.8, ML +1.7, DV −1.9; OB, AP +3.5, ML +1, DV −2.5; striatum, AP +1, ML + 2, DV −3.5; and lateral ventricle, AP −0.3, ML +1, DV −2.6. When indicated, BrdUrd (Boehringer Mannheim), 80 mg/kg in saline, was administered i.p. daily, for 8 days, before killing.

Tissue Processing and Immunohistochemistry. Anesthetized mice were perfused with 0.9% NaCl followed by 4% paraformaldehyde. Brains were equilibrated for 24 h in 30% sucrose in PBS and quick frozen in optimal cutting-temperature compound. Coronal cryostatic sections (20-μm) were blocked in PBS/10% goat serum/0.1% Triton X-100/1% BSA, incubated overnight with primary antibodies at 4°C [mouse monoclonal anti-NeuN, anti-TUJ-1 (Chemicon; 1:1,000) and anti-BrdUrd (Boehringer Mannheim; 2 μg/ml); affinity-purified rabbit anti-GFP (1:100; Molecular Probes), goat anti-doublecortin (Santa Cruz Biotechnology, 1:200), and guinea pig anti-glial fibrillary acidic protein (GFAP; Advanced Immunochemical, Long Beach, CA; 1:500)] and then with FITC and tetramethylrhodamine B isothiocyanate-conjugated secondary antibodies (Molecular Probes; 1:1,000) in blocking solution at room temperature for 2 h, washed, coverslipped in permanent mounting medium, and examined under a Bio-Rad confocal microscope. For the simultaneous detection of BrdUrd and GFP, antigens were unmasked by boiling in 10 mM sodium citrate (pH 6.0) for 5 min. Sections were blocked, incubated with anti-GFP, fixed in 4% paraformaldehyde, incubated in 2 M HCl for 20 min, rinsed in 0.1 M boric acid (pH 8.5) for 10 min, washed, incubated sequentially with FITC goat anti-rabbit antibody, mouse monoclonal anti-BrdUrd, and tetramethylrhodamine B isothiocyanate goat anti-mouse. To quantify labeled cells, the number of BrdUrd- or NeuN-positive nuclei identifiable in a selected optical field was counted, and the fraction of labeled nuclei showing GFP-positive cytoplasm in the same field was assessed. The analysis was performed on three randomly chosen fields taken from two to three nonsequential sections from three mice per experimental group.

Primary Cultures and Population Analysis. Mice were anesthetized with Tribromoethanol 1.25% i.p., their brains were removed, and the SVZ was excised from both hemispheres (treated as separate samples). Tissues pooled from two to three mice were enzymatically and mechanically dissociated, and cells were resuspended in growth factor-free DMEM/F12 medium (control medium) (47). For the neurosphere-forming assay, cells were plated (200 cells per cm^2) in control medium containing epidermal growth factor (20 ng/ml) and basic fibroblast growth factor (FGF2; 10 ng/ml) (Peprotech, Rocky Hill, NY) (growth medium). Primary spheres were counted after 7–12 days *in vitro* and scored under a fluorescence microscope. GFP-positive spheres were manually picked up and pooled. GFP-positive and the remaining GFP-negative spheres were mechanically dissociated and single cells were plated in growth medium. Secondary spheres (counted after 7–12 days) were pooled, mechanically dissociated, and replated in growth medium (3,500 cells per cm^2). This procedure was repeated twice; then cells were replated in growth medium (10^4 cells per cm^2) to generate bulk cultures. Viability was assessed at each passage by trypan blue exclusion. Growth curves were obtained as described (48). Data were interpolated by using a linear regression model and best fitted the equation: $y = a + bx$, where y is the estimated total number of cells (in log scale), x is the time (days *in vitro*), a is the intercept value, and b is the slope. Slope values were compared by using a t test followed by a Bonferroni post hoc test.

To assess multipotentiality an aliquot of cells was collected at progressive subculturing steps and differentiated by plating on matrigel-coated coverslips in the presence of FGF2 (10 ng/ml). After 2 days FGF2 was removed and FCS (2%) was added. After 5 days cells were fixed and processed for immunocytochemistry (see below).

For *in vitro* transduction, NSCs at different subculturing passages were incubated overnight in growth medium with increasing concentrations of LV (3×10^5 to 6×10^6 transducing units^{HeLa} per ml). After 4 days neurospheres were dissociated and replated in growth medium. Cells were analyzed by FACS after 5–7 days. High-molecular-weight DNA was isolated from NSC pelleted at different passages by DNeasy Kit (Qiagen, Valencia, CA), digested overnight with *Bam*HI, and analyzed for WPRE sequence by Southern blot analysis as described (46).

Immunostaining of NSC Cultures. Double-labeling immunofluorescence was performed as described (20, 47). Primary antibodies/antisera were the following: mouse monoclonal anti-microtubule-associated protein 2, anti-galactocerebroside C, and anti-O4 (1:200; Chemicon); anti-Tuj1 (1:400; Covance, Princeton); and rabbit antisera against GFAP (1:300; DAKO). Secondary antibodies were the following: goat anti-mouse or anti-rabbit IgG conjugated with Cy3 (1:1,000; Jackson ImmunoResearch), 7-amino-4-methylcoumarin-3-acetic acid (1:100; Jackson ImmunoResearch) or Alexa 488 (1:1000; Molecular Probes); and Cy3-conjugated donkey anti-mouse IgM (1:100; Jackson ImmunoResearch). Samples were examined by using a Nikon Eclipse 3000 fluorescence microscope. No labeling was observed in the absence of primary antibodies/antisera. The number of cells immunoreactive for different antigens was counted in at least five nonoverlapping fields in each sample, for a total of >500 cells per sample. The total number of cells in each field was determined by counterstaining nuclei with 4,6-diamidine-2-phenylindole dihydrochloride (DAPI, Sigma; 50 μg/ml in PBS for 15 min at room temperature).

Results

***In Vivo* Transduction of Neural Progenitor Cells.** We injected vesicular stomatitis virus-pseudotyped, late-generation LV expressing the GFP (LV-GFP) into the right SVZ of adult mice and analyzed GFP labeling in serial brain sections 2 weeks and 3 and 6 months later. GFP expression in the LVs was driven by the ubiquitously expressed phosphoglycerate kinase promoter and by the posttranscriptional regulatory element of the woodchuck hepadnavirus. Two weeks after injection, numerous GFP+ cells were found in the SVZ and spread in an approximate 1-mm radius from the injection site. At the same time point, few GFP+ cells could be detected in the OB (not shown). Two, 3, and even 6 months after injection, the GFP-labeling pattern in the SVZ was similar to that found after 2 weeks (Fig. 1 *a–c*). GFP was expressed in glial and neuronal cell types, as demonstrated by the presence of GFAP+/GFP+ and TUJ1+/GFP+ cells (Fig. 1 *d* and *e*). More important, at these time points a remarkable density of GFP+ cells was found in the OB ipsilateral to the injection (Fig. 1 *f*, *g*, and *i*). The GFP+ cells were mainly found in the granule cell layer (GCL) with the morphology of granule cells. They also showed prominent dendritic arborization in the external plexiform layer (Fig. 1*h*).

To rule out the possibility that OB labeling resulted from LV-GFP leaking through the cerebroventricular compartment, we injected LV-GFP into the lumen of the right lateral ventricle and monitored GFP-expressing cells throughout the brain after 2 weeks and 2 months. At both times, we observed intense GFP labeling of the ependymal layer throughout the ventricular system but we did not find GFP labeling of subependymal cells. Although GFP expression was maintained in ependymal cells for at least 2 months after injection (Fig. 1*j*), we did not observe GFP labeling in the OB of intraventricularly injected mice (Fig. 1*k*).

Confocal immunofluorescence microscopy showed that the vast majority (98 ± 2%, $n = 3$) of GFP+ cells found in the GCL 3 months after LV injection into the SVZ expressed NeuN (Fig. 1*l*), a nuclear protein associated with terminal neuronal differentiation. Notably, the NeuN+/GFP+ cells represented up to 17% of the total NeuN+ cells in the GCL layer, whereas none of the GFP-expressing cells colabeled with the astrocyte marker

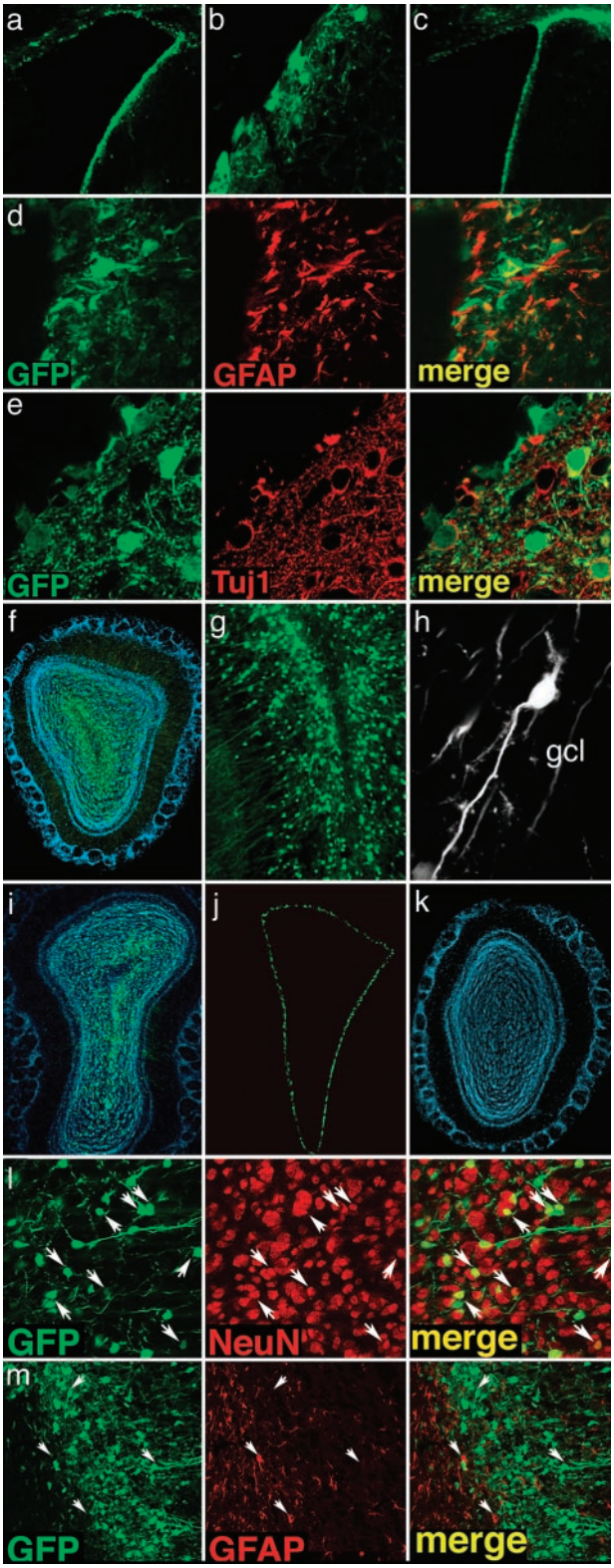

Fig. 1. Long-term marking of SVZ cells by LV. (*a–c*) GFP-expressing LV were unilaterally injected in the forebrain SVZ; brain sections were analyzed 3 (*a* and *b*) and 6 (*c*) months later. GFP expression was evident at the site of injection at both time points (*b*, high-power magnification of *a*). (*d* and *e*) Three months after injection confocal analysis of double-labeled sections showed GFP+ cells (*d* and *e*, green) expressing markers of glial (*d*, GFAP, red) or neural (*e*, Tuj1, red) cells. (*f–i*) Many GFP+ cells with the typical morphology of granule neurons (*g* and *h*) were detected in the OB 2 (*f–h*) and 6 (*i*) months after LV injection in the SVZ. Injection of GFP-expressing LV in the lateral ventricle resulted in intense labeling of the ependymal layer (*j*), but no GFP-expressing cells were detected in the OB of these animals 2 months after injection (*k*, DAPI staining). (*l* and *m*) Double-staining confocal immunofluorescence using antibodies against cell differentiation markers showed that the majority of GFP-expressing cells found in the OB 3 months after LV injection into the SVZ expressed NeuN (*l*, red), whereas no GFP+ cells colabeled with the astrocyte marker GFAP (*m*, red) could be detected. Arrows identify the position of representative cells in the fields. Representative pictures from three mice analyzed per time point.

GFAP (Fig. 1*m*). These results indicate that the progeny of SVZ-transduced cells were observed as neurons in the OB GCL as late as 6 months later.

The observation of GFP+ cells in the OB was specific to SVZ injections. When we injected LV-GFP into the hippocampus or the striatum, GFP+ cells remained confined to the injected area, indicating that LVs do not diffuse long-range within the brain.

The time of appearance and the morphology of GFP+ cells in the OB after LV-GFP injection in the SVZ were consistent with previous data on intra-SVZ administration of retroviral vectors (6, 32, 49). However, differences between those studies and ours suggested that long-lived SVZ progenitors were targeted by LV transduction. In fact, inspection of serial coronal brain sections 3 months after LV-GFP injection showed a significant number of GFP+ cells both in the SVZ and all along the whole RMS, up to its rostral extension into the OB. Cells were specifically confined within the pathway (Fig. 2 *a* and *b*), displayed the typical morphology of young migratory neuroblasts, were not labeled by NeuN antibodies (not shown), and were immunoreactive for the early neuronal markers β-tubulin (Fig. 2*c*) and doublecortin (50) (Fig. 2*d*).

To further investigate the sustained generation of GFP+ cells in the SVZ, we gave an 8-day-long pulse of BrdUrd to mice injected 3 months before with LV in the SVZ and assessed the occurrence of double-labeled BrdUrd+/GFP+ cells (Fig. 2 *e* and *f*). Because the vector was injected 3 months before BrdUrd administration, we can rule out that BrdUrd incorporation might reflect possible DNA repair consequent to LV administration and integration. Confocal analysis showed that a significant fraction of the BrdUrd+ cells in the SVZ ($15 \pm 5\%$, $n = 3$) and in the RMS ($63 \pm 6\%$, $n = 3$) were also GFP+. These results showed that 3 months after transduction by LV-GFP, SVZ cells were still engaged in neurogenesis. Similar results were obtained when applying the same BrdUrd-labeling protocol to mice injected with LV-GFP 6 months earlier (not shown).

Taken together our results showed that a single injection of LV in adult mice SVZ resulted in stable long-term gene expression in the whole SVZ-RMS-OB pathway, indicating that the vector efficiently targeted self-renewing precursors, which most likely belong to the stem-cell pool residing in the SVZ.

Isolation of *In Vivo* Gene-Marked NSCs. To determine whether the SVZ cells transduced *in vivo* by LV comprised self-renewing, multipotent NSCs, we cultured dissociated cells from the SVZ of mice injected with LV-GFP 3 months earlier. Tissues from both the injected (right) and the controlateral (left) hemisphere were dissociated and cultured with mitogens (epidermal growth factor and FGF2) in a neurosphere-forming assay (7, 20, 47) (see *Supporting Text* and Fig. 4 *a* and *b*, which are published as supporting information on the PNAS web site). After 7–12 days similar numbers of spheres per well were generated in cultures from the right and left SVZ region, respectively (29.3 ± 17.9 and 37.5 ± 11.7; mean $\pm$ SD from three independent experiments). From one to seven spheres per well (4–58% of the total) in the cultures from LV-injected SVZ expressed GFP, essentially in all the cells within the sphere (Fig. 4 *c–e*). GFP-expressing spheres were not observed in cultures derived from noninjected tissues.

GENETICS

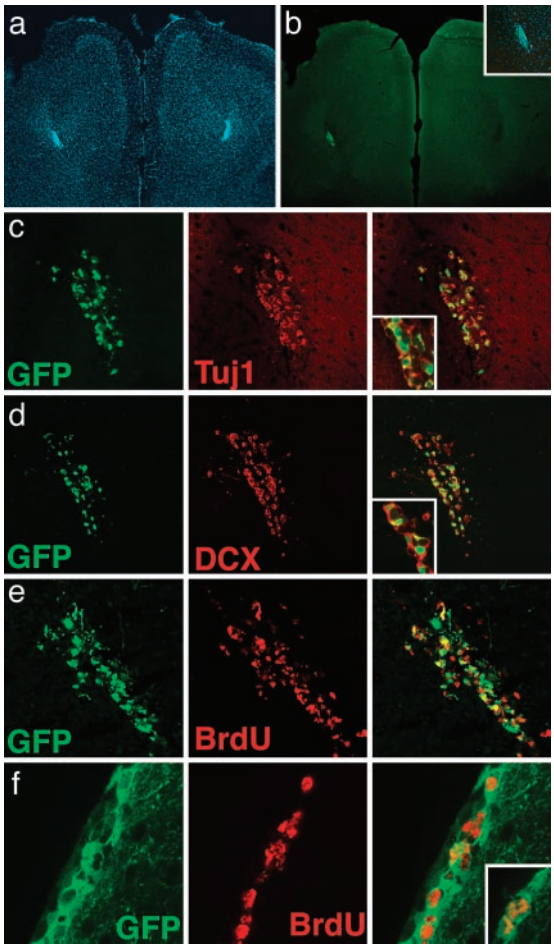

Fig. 2. GFP-positive neuroblasts were observed in the RMS 3 and 6 months after LV-GFP injection. Photograph shows migrating GFP+ cells in the RMS 3 months after injection in the SVZ (*a*, DAPI staining, blue; *b*, GFP, green). Confocal immunofluorescence microscopy showed that many of the GFP+ migrating cells expressed the early neuronal markers Tuj1(*c*, red) and doublecortin (DCX; *d*, red). *Insets* show higher magnification pictures of the double-labeled cells. *e* and *f* show RMS and SVZ from mice administered BrdUrd for 8 days, starting 3 months after LV-GFP injection in the SVZ and stained for BrdUrd (red) and GFP (green). Cells stained for both BrdUrd and GFP appear yellow in the merged picture. Inset in *f* shows nuclei staining for BrdUrd. Representative pictures from three mice analyzed per time point.

To test self-renewal of the LV-transduced, neurosphere-forming cells, GFP-expressing primary spheres were collected, dissociated to single cells, and replated under identical conditions. Many of these cells formed secondary spheres, which were subcultured to tertiary spheres, still expressing GFP in all the cells within the sphere (Fig. 4 *f* and *g*). In three independent experiments we obtained increasing numbers of secondary and tertiary spheres, starting from six, three, and two GFP-expressing primary neurospheres, respectively.

These results indicated that some of the precursor cells transduced *in vivo* by LV-GFP displayed self-renewal properties *in vitro*. To distinguish between transiently dividing progenitors, which may retain a limited self-renewal capacity, and stem cells, which display long-term self-renewal and multilineage differentiation potential (51), we performed a long-term population analysis (up to 6 months) of cultures established from GFP+ primary neurospheres. Cultures from noninjected SVZ were used as control. We also established a GFP+ clonal cell line that was maintained up to the 33th passage. The GFP+ cells consistently expanded in number over time, displaying long-term self-renewal capacity, with proliferation remaining strictly dependent on the presence of mitogens (Fig. 3*a*). FACS analysis showed that virtually all cells expressed GFP to a similar high mean fluorescent intensity (MFI; Fig. 3*b*), whereas the narrow distribution of GFP MFI was indicative of the clonal nature of this population. In fact, when SVZ-derived NSC isolated from the noninjected SVZ were transduced *in vitro* with LV-GFP (from 3×10^5 to 6×10^6 transducing units/ml), the GFP+ cells showed a much broader distribution, reflecting the random vector integration in cultured cells (Fig. 3*c*). Southern analysis of cellular DNA extracted at different subculturing passages (Fig. 3*d*) showed a unique vector integration pattern and the presence of a high number of vector copies per cell genome. These two features remained unchanged upon long-term culturing.

Removal of epidermal growth factor and FGF2 at all subculturing passages tested triggered cell differentiation to yield cells with neuronal, astrocytic, and oligodendrocytic phenotypes, as assessed by immunostaining for lineage-specific markers (Fig. 3 *e–m*). Quantitative analysis of microtubule-associated protein 2-, Tuj1-, GFAP-, galactocerebroside C-, and O4-positive cells in the cultures is summarized in Table 1, which is published as supporting information on the PNAS web site.

Taken together these results indicated that long-lived neural precursors transduced by LV in the adult mouse SVZ were multipotent NSCs with long-term self-renewal capacity in culture.

Discussion

Stable and efficient gene transfer into multipotent stem cells is crucial for developmental studies and therapeutic applications. Here, we showed efficient gene transfer into long-lived, primary neural precursors of the adult SVZ *in vivo* by advanced-generation LVs, and long-term transgene expression both in migrating neuroblasts, throughout the SVZ-RMS pathway, and in newly generated neurons in the OB. In *ex vivo* culture, a fraction of LV-transduced cells displayed multipotentiality and long-term self-renewal at both clonal and population levels. These findings indicated that self-renewing NSCs in the SVZ were targeted by LVs.

The time of appearance and the phenotype of gene-marked cells in the OB were consistent with previous studies using alternative approaches to monitor SVZ-dependent OB neurogenesis (6, 32, 46, 50). Unlike gamma-retroviral and adenoviral vectors, LVs allowed for high-efficiency gene marking and long-term expression throughout the SVZ-RMS-OB region. LV effectiveness is most likely due to the mitosis-independent integration of these vectors into the genome of target cells. Although LVs efficiently transduce postmitotic neurons and other differentiated cell types *in vivo* (52), some resting cells such as T lymphocytes and hematopoietic stem cells are resistant or poorly susceptible to transduction, respectively (53, 54). However, progression of these cells into the G_1 phase of the cell cycle is sufficient to allow efficient transduction (55–58). These properties of LV may enable efficient gene transfer into SVZ NSCs. In fact, these primary precursors show characteristics of resting or slowly proliferating astrocytes (B cells), that are poorly susceptible to gamma-retroviral infection (7, 49). Effective marking of NSCs was best indicated by the fact that, 2 and even 6 months after vector injection, a significant fraction (up to 63%) of the proliferating neuroblasts in the RMS expressed GFP. The time required for newly generated SVZ neuroblasts to reach the OB is ≈9 days. At that time, the cells move from the OB core to the cortical layers and, by 3 weeks after their birth in the SVZ, they acquire their mature morphology (49). If LV injected into the SVZ had transduced only migratory neuroblasts (A cells), the latter would have cleared the original site of infection and the RMS well ahead of the time of our long-term analysis, as observed in previous studies with gamma-retroviral vectors (49, 59). The detection of typical chains of GFP+ neuroblasts all

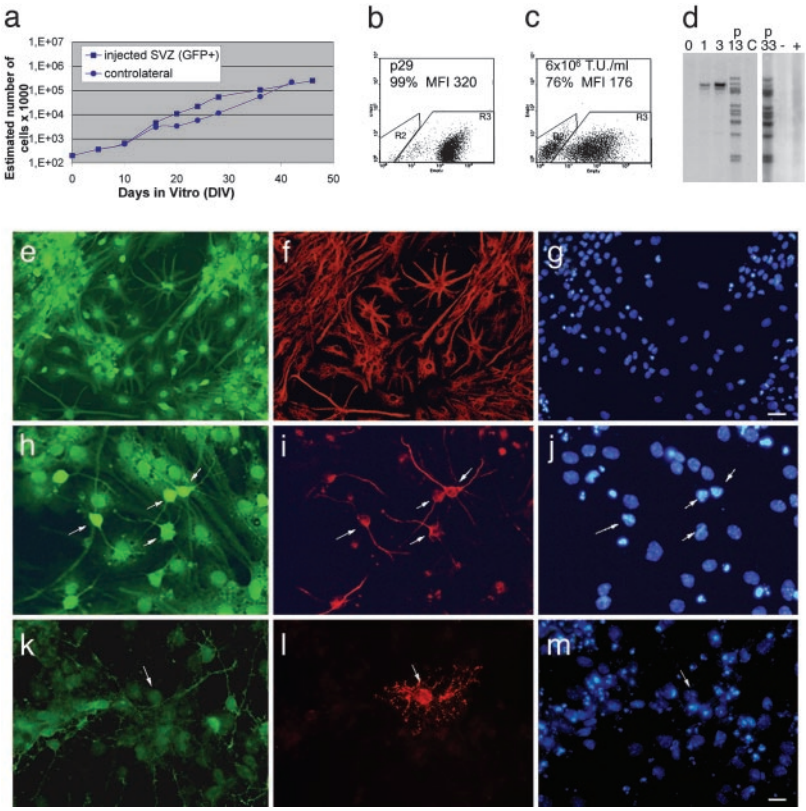

Fig. 3. SVZ cells targeted *in vivo* by LV display features of multipotent NSCs in culture. (*a*) Growth curves for cell lines (passages 6–15) derived from the injected SVZ (GFP+, squares) or controlateral SVZ (GFP−, circles). The slope values ± SE ($b = 0.07389 \pm 0.00588$ and 0.07132 ± 0.0039 for GFP+ and GFP− cells, respectively) showed no significant difference ($P = 0.8$). Data shown are from one of three independent cultures with similar results. DIV, days *in vitro*. (*b* and *c*) Cytofluorimetric analysis of NSCs from LV-injected SVZ (passage 29; *b*) and from noninjected SVZ after *in vitro* transduction with LV-GFP (6×10^6 transducing units (T.U.)/ml) (*c*). The frequency and MFI of GFP+ cells are indicated. (*d*) Southern analysis of DNA extracted from *ex vivo* expanded GFP+ NSCs showing a unique integration pattern (lanes: 0, negative control; 1 and 3, plasmid standards for one and three vector copies per genome; p13 and p33, GFP+ cells from injected SVZ, at passages 13 and 33; C, noninfected NSCs). Each band corresponds to one vector copy per genome. The same analysis performed on *in vitro* transduced NSCs (same cells shown in *c*) showed random LV integration (lanes: + and −, transduced and nontransduced cells, respectively). (*e–m*) Stable GFP expression and multipotency of NSC cultures from LV-injected SVZ; upon mitogens removal, clonally derived cells gave rise to GFAP+ astrocytes (*e–g*), TUJ1+ neurons (*h–j*), and O4+ oligodendrocytes (*k–m*). GFP in green (*e*, *h*, and *k*), GFAP- (*f*), TUJ1− (*i*), and O4-positive cells (*l*) in red; nuclei stained with DAPI (*g*, *j*, and *m*) in blue. Arrows identify the same cells in the field. (Magnification, *e–g*, ×200; *h–m*, ×400.) [Bars, *e–g*, 30 μm (in *g*); *h–m*, 20 μm (in *m*)].

along the SVZ-RMS pathway, 3 and even 6 months after LV injection, showed that gene-marked neuroblasts were still being produced by transduced cells within the SVZ at these late times. Migratory neuroblasts are produced through type C precursors, which are rapidly dividing transit-amplifying cells (60); thus, the injection of LV into the SVZ must have targeted long-lived progenitors, i.e., type B astrocytes, that are classified as NSCs (6). Support for this conclusion comes from the detection of GFP-labeled cells coexpressing GFAP in the SVZ analyzed at late times after LV injection.

The absence of GFP labeling of SVZ cells after intraventricular LV injection and ependymal marking show that LVs, as shown also for adenoviral vectors (61), could access the SVZ neurogenic progenitor pool only from the adluminal side of the ependyma and that these progenitors do not derive from ependymal cells.

Classically, as it has been established for the hematopoietic system, stable repopulation by gene-marked cells of a cell lineage or tissue compartment undergoing rapid turnover provides the most stringent criteria for the existence and genetic marking of long-term self-renewing stem cells. Although self-renewal of NSCs is difficult to demonstrate *in vivo*, previous reports suggested that SVZ type B astrocytes could behave as self-renewing precursors (6). Our findings provide strong experimental support to this notion, demonstrating not only that SVZ primary precursors undergo long-term self-renewal *in vivo* but also that they can be genetically modified *in vivo* in a stable and efficient manner. A direct implication of our gene transfer strategy is that the effect of the initial transduction of NSCs is amplified by their continuous neurogenic activity and the production of transduced progeny that migrate away from the injection site and distribute into the mature brain parenchyma.

That NSCs were targeted *in vivo* by LVs was further substantiated by culturing experiments demonstrating that some of the transduced SVZ cells behaved as multipotent, long-term self-renewing precursors *in vitro*. Under selective culture conditions, some of the GFP-expressing cells isolated from SVZ injected with LV 2 months before gave rise to primary neurospheres that were capable of generating clonal secondary and tertiary neurospheres, thus showing self-renewal capacity. The long-term self-renewal and the stable developmental potential of the GFP-transduced cells were formally proven by population and clonal analysis in cultures established from GFP-expressing primary neurospheres. The cells displayed a stable rate of expansion for up to 6 months in culture (the latest time tested) and, upon growth factor withdrawal, generated cells with neuronal, astrocytic, and oligodendrocytic phenotype at each subculturing step tested. It is likely that some of the GFP+ primary neurospheres were generated from transit-amplifying precursors (C cells) that revert to multipotent stem cells when cultured *in vitro* in the presence of epidermal growth factor (62). However, because our primary cultures were established from SVZ injected with LV 3 months before, GFP-expressing C cells present in those tissues could only derive from previously transduced type B precursors.

The finding of unique vector integration patterns in the DNA of the GFP+ cells in our combined *in vivo*/*in vitro* experiments accounted for their clonal origin. The cells shown in Fig. 3 carried 13 vector copies in the genome. Although this finding proved the high efficiency of gene transfer achieved by LV *in vivo*, it may raise concerns as to the possible genotoxicity of multicopy vector integration and its possible contribution to establishing long-term cultures in our experiments. These *ex vivo* isolated cells, however, retained stable growth rate, growth factor-dependence, and normal differentiation behavior upon mitogen removal. Furthermore, on implantation into the brain of newborn mice, they dispersed into the host tissue acquiring the morphology of neuronal and glial cells, without obvious signs of any transformed behavior (see *Supporting Text* and Fig. 5, which are published as supporting information on the PNAS web site). Whether such high levels of gene transfer are safe and appropriate for future therapeutic applications in addition to basic experimental studies remains to be determined. Nonetheless, the

possibility of achieving multiple integrations per cell *in vivo* may permit high levels of transgene expression, and, in conjunction with the coadministration of different LV, exogenous regulation of transgene expression and expression of multiple transgene combinations.

The vectors and gene transfer strategies described in this work will not only allow performing novel semiquantitative and long-term studies on adult NSC physiology, but also provide the means to introduce therapeutic genes in these cells and to explore novel strategies for the treatment of several types of CNS diseases.

We thank C. Panzeri and R. Summers for assistance in confocal microscopy, A. Mallamaci and L. Muzio for reagents and advice, and H. Suh for critical review of the manuscript. This research was supported by Telethon Grants B58 (to L.N.), E.1246 (to A.L.V.), and GGP030245 (to A.G.), Telethon Institute of Gene Therapy (L.N.), BMW Italy (A.L.V.), European Union Grant QLRT-2001-02114 (to L.N.), (N)europark (L.N.), Italian Ministry of Scientific Research and of Health (P. N. Cellule Staminali) awards (to L.N. and A.L.V.), and National Institutes of Health, National Institute on Aging, and National Institute of Neurological Disease and Stroke grants (to F.H.G.). A.C. received a Telethon postdoctoral fellowship.

1. Altman, J. (1962) *Science* **135,** 1127–1128.
2. Altman, J. (1969) *J. Comp. Neurol.* **137,** 433–457.
3. Eriksson, P. S., Perfilieva, E., Bjork-Eriksson, T., Alborn, A. M., Nordborg, C., Peterson, D. A. & Gage, F. H. (1998) *Nat. Med.* **4,** 1313–1317.
4. Gage, F. H. (2000) *Science* **287,** 1433–1438.
5. Alvarez-Buylla, A., Seri, B. & Doetsch, F. (2002) *Brain Res. Bull.* 57, 751–758.
6. Doetsch, F., Caille, I., Lim, D. A., Garcia-Verdugo, J. M. & Alvarez-Buylla, A. (1999) *Cell* **97,** 703–716.
7. Morshead, C. M., Reynolds, B. A., Craig, C. G., McBurney, M. W., Staines, W. A., Morassutti, D., Weiss, S. & van der Kooy, D. (1994) *Neuron* **13,** 1071–1082.
8. Kaplan, M. S. & Bell, D. H. (1984) *J. Neurosci.* **4,** 1429–1441.
9. Cameron, H. A., Woolley, C. S., McEwen, B. S. & Gould, E. (1993) *Neuroscience* **56,** 337–344.
10. Gage, F. H., Kempermann, G., Palmer, T. D., Peterson, D. A. & Ray, J. (1998) *J. Neurobiol.* **36,** 249–266.
11. Doetsch, F. & Alvarez-Buylla, A. (1996) *Proc. Natl. Acad. Sci. USA* **93,** 14895–14900.
12. Jankovski, A. & Sotelo, C. (1996) *J. Comp. Neurol.* **371,** 376–396.
13. Luskin, M. B. (1993) *Neuron* **11,** 173–189.
14. Lois, C., Garcia-Verdugo, J. M. & Alvarez-Buylla, A. (1996) *Science* **271,** 978–981.
15. Song, H. J., Stevens, C. F. & Gage, F. H. (2002) *Nat. Neurosci.* **5,** 438–445.
16. Kempermann, G., Gast, D., Kronenberg, G., Yamaguchi, M. & Gage, F. H. (2003) *Development (Cambridge, U.K.)* **130,** 391–399.
17. Ahmed, S., Reynolds, B. A. & Weiss, S. (1995) *J. Neurosci.* **15,** 5765–5778.
18. Aberg, M. A., Aberg, N. D., Palmer, T. D., Alborn, A. M., Carlsson-Skwirut, C., Bang, P., Rosengren, L. E., Olsson, T., Gage, F. H. & Eriksson, P. S. (2003) *Mol. Cell Neurosci.* **24,** 23–40.
19. Johe, K. K., Hazel, T. G., Muller, T., Dugich-Djordjevic, M. M. & McKay, R. D. (1996) *Genes Dev.* **10,** 3129–3140.
20. Gritti, A., Frolichsthal-Schoeller, P., Galli, R., Parati, E. A., Cova, L., Pagano, S. F., Bjornson, C. R. & Vescovi, A. L. (1999) *J. Neurosci.* **19,** 3287–3297.
21. Hsieh, J., Aimone, J. B., Kaspar, B. K., Kuwabara, T., Nakashima, K. & Gage, F. H. (2004) *J. Cell Biol.* **164,** 111–122.
22. Johansson, C. B., Momma, S., Clarke, D. L., Risling, M., Lendahl, U. & Frisen, J. (1999) *Cell* **96,** 25–34.
23. Chiasson, B. J., Tropepe, V., Morshead, C. M. & van der Kooy, D. (1999) *J. Neurosci.* **19,** 4462–4471.
24. Capela, A. & Temple, S. (2002) *Neuron* **35,** 865–875.
25. Lim, D. A., Tramontin, A. D., Trevejo, J. M., Herrera, D. G., Garcia-Verdugo, J. M. & Alvarez-Buylla, A. (2000) *Neuron* **28,** 713–726.
26. Doetsch, F. (2003) *Curr. Opin. Genet. Dev.* **13,** 543–550.
27. Kempermann, G., Kuhn, H. G. & Gage, F. H. (1997) *Nature* **386,** 493–495.
28. van Praag, H., Kempermann, G. & Gage, F. H. (2000) *Nat. Rev. Neurosci.* **1,** 191–198.
29. Szele, F. G. & Chesselet, M. F. (1996) *J. Comp. Neurol.* **368,** 439–454.
30. Moreno-Lopez, B., Noval, J. A., Gonzalez-Bonet, L. G. & Estrada, C. (2000) *Brain Res.* **869,** 244–250.
31. Nait-Oumesmar, B., Decker, L., Lachapelle, F., Avellana-Adalid, V., Bachelin, C. & Van Evercooren, A. B. (1999) *Eur. J. Neurosci.* **11,** 4357–4366.
32. Carleton, A., Petreanu, L. T., Lansford, R., Alvarez-Buylla, A. & Lledo, P. M. (2003) *Nat. Neurosci.* **6,** 507–518.
33. van Praag, H., Schinder, A. F., Christie, B. R., Toni, N., Palmer, T. D. & Gage, F. H. (2002) *Nature* **415,** 1030–1034.
34. Song, H., Stevens, C. F. & Gage, F. H. (2002) *Nature* **417,** 39–44.
35. Craig, C. G., Tropepe, V., Morshead, C. M., Reynolds, B. A., Weiss, S. & van der Kooy, D. (1996) *J. Neurosci.* **16,** 2649–2658.
36. Kuhn, H. G., Winkler, J., Kempermann, G., Thal, L. J. & Gage, F. H. (1997) *J. Neurosci.* **17,** 5820–5829.
37. Aberg, M. A., Aberg, N. D., Hedbacker, H., Oscarsson, J. & Eriksson, P. S. (2000) *J. Neurosci.* **20,** 2896–2903.
38. Zigova, T., Pencea, V., Wiegand, S. J. & Luskin, M. B. (1998) *Mol. Cell Neurosci.* **11,** 234–245.
39. Fallon, J., Reid, S., Kinyamu, R., Opole, I., Opole, R., Baratta, J., Korc, M., Endo, T. L., Duong, A., Nguyen, G., *et al.* (2000) *Proc. Natl. Acad. Sci. USA* **97,** 14686–14891.
40. Nakatomi, H., Kuriu, T., Okabe, S., Yamamoto, S., Hatano, O., Kawahara, N., Tamura, A., Kirino, T. & Nakafuku, M. (2002) *Cell* **110,** 429–441.
41. Naldini, L., Blomer, U., Gage, F. H., Trono, D. & Verma, I. M. (1996) *Proc. Natl. Acad. Sci. USA* **93,** 11382–11388.
42. Regulier, E., Pereira de Almeida, L., Sommer, B., Aebischer, P. & Deglon, N. (2002) *Hum. Gene Ther.* **13,** 1981–1990.
43. Baekelandt, V., Claeys, A., Eggermont, K., Lauwers, E., De Strooper, B., Nuttin, B. & Debyser, Z. (2002) *Hum. Gene Ther.* **13,** 841–853.
44. Consiglio, A., Quattrini, A., Martino, S., Bensadoun, J. C., Dolcetta, D., Trojani, A., Benaglia, G., Marchesini, S., Cestari, V., Oliverio, A., *et al.* (2001) *Nat. Med.* **7,** 310–316.
45. Georgievska, B., Kirik, D., Rosenblad, C., Lundberg, C. & Bjorklund, A. (2002) *NeuroReport* **13,** 75–82.
46. Follenzi, A., Ailles, L. E., Bakovic, S., Geuna, M. & Naldini, L. (2000) *Nat. Genet.* **25,** 217–222.
47. Gritti, A., Parati, E. A., Cova, L., Frolichsthal, P., Galli, R., Wanke, E., Faravelli, L., Morassutti, D. J., Roisen, F., Nickel, D. D. & Vescovi, A. L. (1996) *J. Neurosci.* **16,** 1091–1100.
48. Gritti, A., Bonfanti, L., Doetsch, F., Caille, I., Alvarez-Buylla, A., Lim, D. A., Galli, R., Verdugo, J. M., Herrera, D. G. & Vescovi, A. L. (2002) *J. Neurosci.* **22,** 437–445.
49. Petreanu, L. & Alvarez-Buylla, A. (2002) *J. Neurosci.* **22,** 6106–6113.
50. Brown, J. P., Couillard-Despres, S., Cooper-Kuhn, C. M., Winkler, J., Aigner, L. & Kuhn, H. G. (2003) *J. Comp. Neurol.* **467,** 1–10.
51. Potten, C. S. & Loeffler, M. (1990) *Development (Cambridge, U.K.)* **110,** 1001–1020.
52. Vigna, E. & Naldini, L. (2000) *J. Gene Med.* **2,** 308–316.
53. Korin, Y. D. & Zack, J. A. (1999) *J. Virol.* **73,** 6526–6532.
54. Sutton, R. E., Reitsma, M. J., Uchida, N. & Brown, P. O. (1999) *J. Virol.* **73,** 3649–3660.
55. Uchida, N., Sutton, R. E., Friera, A. M., He, D., Reitsma, M. J., Chang, W. C., Veres, G., Scollay, R. & Weissman, I. L. (1998) *Proc. Natl. Acad. Sci. USA* **95,** 11939–11944.
56. Cavalieri, S., Cazzaniga, S., Geuna, M., Magnani, Z., Bordignon, C., Naldini, L. & Bonini, C. (2003) *Blood* **102,** 497–505.
57. Ducrey-Rundquist, O., Guyader, M. & Trono, D. (2002) *J. Virol.* **76,** 9103–9111.
58. Ailles, L., Schmidt, M., Santoni de Sio, F. R., Glimm, H., Cavalieri, S., Bruno, S., Piacibello, W., Von Kalle, C. & Naldini, L. (2002) *Mol. Ther.* **6,** 615–626.
59. Lois, C. & Alvarez-Buylla, A. (1994) *Science* **264,** 1145–1148.
60. Doetsch, F., Garcia-Verdugo, J. M. & Alvarez-Buylla, A. (1999) *Proc. Natl. Acad. Sci. USA* **96,** 11619–11624.
61. Yoon, S. O., Lois, C., Alvirez, M., Alvarez-Buylla, A., Falck-Pedersen, E. & Chao, M. V. (1996) *Proc. Natl. Acad. Sci. USA* **93,** 11974–11979.
62. Doetsch, F., Petreanu, L., Caille, I., Garcia-Verdugo, J. M. & Alvarez-Buylla, A. (2002) *Neuron* **36,** 1021–1034.